Nanoscience and Nanometrology
2017; 3(1): 12-19
http://www.sciencepublishinggroup.com/j/nsnm
doi: 10.11648/j.nsnm.20170301.13
ISSN: 2472-3622 (Print); ISSN: 2472-3630 (Online)

Synthesis of SnO_2 Nanopowders for Advanced Ceramics and Electronic Sensor Transducer Devices and Characterization and Band Gap

Rexona Khanom[1, *], Mohammad Anwar Arfien Khan[1], Abdul Gafur[1, 2], Shakila Akter[1, 2, 3], Shamim Ahmed[1, 2, 3], Mohammad Shahjahan[1, 2, 3, 4], Mohammad Raqibul Qadir[1, 2]

[1]Institute of Glass and Ceramic Research and Testing, Bangladesh Council of Scientific and Industrial Research, Dhanmondi, Dhaka, Bangladesh

[2]Pilot Plant and Process Development Center, Bangladesh Council of Scientific and Industrial Research, Dhanmondi, Dhaka, Bangladesh

[3]Institute of National Analytical and Research Service, Bangladesh Council of Scientific and Industrial Research, Dhanmondi, Dhaka, Bangladesh

[4]BCSIR Laboratories, Dhaka, Bangladesh Council of Scientific and Industrial Research, Dhanmondi, Dhaka, Bangladesh

Email address:

Rexonakhanom@yahoo.com (R. Khanom)

[*]Corresponding author

To cite this article:

Rexona Khanom, Mohammad Anwar Arfien Khan, Abdul Gafur, Shakila Akter, Shamim Ahmed, Mohammad Shahjahan, Mohammad Raqibul Qadir. Synthesis of SnO_2 Nanopowders for Advanced Ceramics and Electronic Sensor Transducer Devices and Characterization and Band Gap. *Nanoscience and Nanometrology.* Vol. 3, No. 1, 2017, pp. 12-19. doi: 10.11648/j.nsnm.20170301.13

Received: March 7, 2017; **Accepted**: May 9, 2017; **Published**: May 22, 2017

Abstract: Reverse Microemulsion Precipitation" was firstly developed for synthesizing SnO_2 nanopowders were intended to as advanced structural materials and hazardous gases, particulates (Pb, Cd, Hg) sensing nanofabricated devices: sensor, transducer, MOSFET, electrodes. Prepared controlled nanopowders were encapsulated with oil phases in spherical water pole at water to surfactant mole ratio w_0=8 and w_0=10. Characteristic absorption of semiconductor at 303.4 nm and no absorption in higher λ and absorption edge in the 321.6-371.6 nm and band gap energy (3.6eV) were observed by UV-Vis measurement confirmed $2SnO_2.4H_2O$ nanoparticles is semiconductor. Sn-O stretching band at 678.94 cm^{-1} and no other groups presence confirmed complete removal of adsorbed chemicals in the course of calcination at 600°C about 4.0 hours from FTIR spectrum. XRD investigation found out phase pure tetragonal SnO_2 nanocrystalline structures and average crystalline size 0.2380 nm at w_0=8. SEM images exhibited spherical morphology counting average particle size 153.242 nm and 131.604 nm and average diameter 8.02 nm at w_0=8 and 10.01 nm at w_0=10 respectively. Higher specific surface area was observed 107.731 m^2/ g (count 637) more than 86.314 m^2/ g (count 341) of relatively larger diameter which is more pronounced compared to ordinary Reverse Microemulsion Method. Findings and standards established this synthesis method as suitable for obtaining the higher degree of surface area and finest crystallinity.

Keywords: SnO_2 Nanopowders, Synthesis, Reverse Microemulsion Precipitation, Characterization, Band Gap Determination

1. Introduction

The chemical synthesis and characterization of SnO_2 nanopowders have received revolutionary attention from many researchers in diversified areas in worldwide [1]. SnO_2 is used as representative nanopowders and n-type semiconductor with high band gap 3.6 eV [2]. Since its high band gap, low electrical and magnetic properties, nano SnO_2 powders are used in several electronic applications as insulators, semiconductors and magnets, thin film etc. Regarding for its unique optical properties, it can be considered in transparent glass ceramics, transparent

windows, transparent electrodes for solar cells, photoconductive devices in LCD, gas charging display, lithium ion batteries [3]. Due to brittleless, stretchable, high mechanical and thermal stress, the basic raw materials of automotive engines, cutting tools, flexible superconducting wire and fiber-optic connector components, wear and scratch resistant parts and watch glasses and ceramic coatings, ceramic membranes so on can be prepared and nanoceramic powders constitute an important segment of the whole national, international nanostructured market [4-6]. Because of antimicrobial, antifungal, antiviral properties, it is found to be used as bio-medical purposes e.g. bone grafting, dental implants, in normal water filter and ultra-pure water filter [7]. Moreover all of these aspects, its more efficient application found to be in nanofabricated sensor of environmentally hazardous gases (CH_4, CO, H_2S, CO_2, NO_2), pollutants and particulates (Pb, Cd, Hg) [8]. For the efficiency of above mentioned products, nanosized SnO_2 nanopowders preparation method with high surface area is concerned [9].

Surplus research journals on synthesis and characterization of SnO_2 nanopowders found in literature till to date [10-11]. However there are few research papers available on advanced ceramics with SnO_2 nanopowders and on environmentally hazardous gases, particulates (Pb, Cd, Hg) sensor, transducer etc. devices. Many reported methods have been derived and employed to produce nano-scale SnO_2 materials in literature are microemulsions, sol-gel, high-energy ball milling, ultrasound, microwave irradiations, spray pyrolysis, direct strike precipitation, hydrothermal, chemical vapor deposition, laser synthesis, and self–propagating high–temperature synthesis, carbothermal reduction, plasma processes, solid-state reaction-thermal oxidation, solvothermal, aerosol flame deposition, polymerizing–complexing sol– gel method, polyol, oxidation, one step solid state synthesis, molten salt synthesis etc. [1-2, 12-13, 8, 14- 18]. Various shapes of SnO_2 nanopowders e.g. spherical, nanotubes, nanotriangles, nanorods, hollow shperes, wormholes etc. have been observed in literature [19]. The enhance crystallinity and high surface area are of great importance and determinant for above mentioned products, method of synthesis should be developed.

In this work, method "Reverse Microemulsion Precipitation" was developed for synthesizing powders of SnO_2 nanoparticles are aimed to get overview of semiconductor of advanced ceramics components, structural materials, coatings and deserved for hazardous gases, particulates (Pb, Cd, Hg) sensing nanofabricated electronic devices: sensor**,** MOSFET, transducer etc. and provide to suppliers of advanced ceramic and structural raw materials, companies involved in R & D and commercialization and chemical companies interested in diversification. The nanopowders were synthesized taking w/o microemulsion as a microreactor. The characterization performed by UV-Vis Spectrophotometer, FTIR, XRD, SEM and the findings were studied comprehensively and to get insight of nanosizesd SnO_2 nanopowders herein.

2. Materials and Methods

2.1. Materials

Cetyltrimethylammoniumbromide (CTAB), cyclohexane, 1-butanol were received without further purifications from Merck Germany. Precursor Tin (IV) Chloride Pentahydrate ($SnCl_4$.5H2O) (s), NH_4OH (25%) solution and acetone were used from Merck Germany. Double distilled deionized water was used for cleaning and all preparations.

2.2. Synthesis

Reverse microemulsions given in Table 1 at water to surfactant mole ratio, w_0=8 and w_0=10 were considered to be prepared by composed of and homogeneously mixing up cetyltrimethylammoniumbromide (CTAB), cyclohexane, 1-butanol and de-ionized water using Microprocess controlled bench-top Ultrasonic Cleaner (model no. powersonic 410). Equal amounts of microemulsions at w_0=8 were placed in two beakers and prepared 0.1M $SnCl_4$ solutions were injected into one beaker by pipettes and Microlitre Syringes (Hamilton Bonadus AG)) and NH_4OH (25%) solution directly incorporated into another beaker using pipettes until pH=12. Followed by homogeneous mixing of solutions of two beakers and pouring precipitating agent NH_4OH solution until complete formation of $2SnO_2.4H_2O$ nanoparticles (opaque appearance) and reached maximum solubility of $2SnO_2.4H_2O$ nanoparticles at pH=12 (until dark blue). Microemulsion at w_0=10, mentioned process was done.

Thus prepared solution was flocculating by adding acetone and kept overnight for settledown of white precipitates of $2SnO_2.4H_2O$ and focused on centrifuging of upper chemicals: NH_4Cl (aq), CTAB, cyclohexane thoroughly by droppers or in a superspeed centrifuge at 8500rpm or 10000rpm if available. The achieved hydroxide precipitates were washing using acetone and dried 24h in oven at 100^0C to eliminate excess CTAB. The resulting precipitates proceed for calcination in Furnace (Nabertherm, geprufte Sicherheit) at 600^0C for about 4 h to exhaust adsorbed chemicals and entirely conversion to SnO_2 nanopowders. The whole process was repeated at three times to obtain constant weight of SnO_2 nanopowders. Microemulsion at w_0=10, mentioned process was done. The method followed the reaction:

$$2\ SnCl_4\,(aq) + 8NH_4OH\,(aq) \rightarrow 2SnO_2.4H_2O\ (\downarrow) + 8NH_4^+\,(aq) + 8Cl^-\,(aq)$$

$$\downarrow$$

$$SnO_2\ (\downarrow) + H_2O\ (\uparrow)$$

This method of synthesis was established on the basis of citation of references of characterization by XRD, UV-Vis Spectrophotometer, FTIR and SEM results consistent with standard SnO_2 nanopowders and commercial sample SnO_2 nanopowders. Commercial SnO_2 nanoparticles (SkySpring Nanomaterials, Inc., 50-70 nm) were characterized using the same techniques in the reported literature [20].

2.3. Characterization: (ASTM Standard Reference: Terminology for E2589-11 and Practices for E2651-13)

Optical transparency in the visible region (higher wavelength) and characteristic absorption in the UV region (short wavelength) of $2SnO_2.4H_2O$ nanoparticles in solution were scanned by using UV-Visible spectrophotometer (Shimadzu, model no.1650) and microemulsion (blank) of same composition used as reference solution and spectra was taken in the range 300-800 nm. XRD (Bruker D8 Advance) was subjected to characterize phase purity, shape, nanocrytalline structure and average crystalline size calculated using Debye-Scherrer relation and the diffraction pattern was recorded at 2θ:20^0-70^0 using a CuKα1 radiation λ = 1.54060Å having Ni filter. The analysis of morphology (size and shape) was run out by conducting Scanning Electron Microscopy, SEM (Hitachi, model no. 33400). SEM was kept on about 12 hours before to measure. The % transmittance of SnO_2 nanopowders after calcination was traced in the wavenumber range 550-4000 cm^{-1} by operating automated FT-IR (Shimadzu, model no. iRaffinity-1) with a resolution of 4 cm^{-1}.

Table 1. *Composition of prepared reverse microemulsion for synthesis SnO2 nanopowders.*

No.	% wt.	% wt.	% wt.	% wt.	w_0
	CTAB	1-butanol	cyclohexane	water	
1.	30	46.2	12	11.8	8
2.	30	43.2	12	11.8	10

3. Results and Discussion

The UV-visible spectrum of $2SnO_2.4H_2O$ nanoparticles in solution at water to surfactant mole ratio w_0=8 is to have presented in Figure 1 and displayed an intense characteristics absorption in the 303.4 nm wavelength range and an absorption edge between 321.6 nm and 371.6 nm and thus being have higher energy in consequence of the relatively larger photon energy than band gap energy to excite and transfer an electron to conduction band from valance band. These findings agree well with literatures [21-22]. However, the band gap energy of SnO_2 nanopowders was calculated by UV-Vis measurement and using Tauc relation [11]:

$$(\alpha h\upsilon)^2 = A\,(h\upsilon - Eg) \qquad (1)$$

where, Eg is the band gap energy and α is the optical absorption coefficient for nanoparticles.

At wavelength 277.80 nm and absorbance 2.383

For nanoparticles $I / I_0 = 10^{\alpha l}$

$$\alpha = 2.383\ cm^{-1}$$

$$h\upsilon\ (eV) = hc / \lambda = 1.24 / \lambda\ (\mu m)$$

$$(\alpha\, h\, \upsilon)^2 = (2.383\ cm^{-1} \times 1.24 / 277.80 \times 10^{-3}\ \mu m)^2$$

$$= 113.167\ cm^{-2}\, eV^2$$

Similarly, calculated values for others wavelength is given in Table 2.

A plot of $(\alpha h\upsilon)2$ versus $h\upsilon$ called Tauc Plot shows linear region, the extrapolation of the curve gives Eg = 3.6 eV from the intersect of the $h\upsilon$ axis inserted in Figure 2 and excellent agreement with the standard Eg of SnO_2 nanoparticles and literatures [3].

The XRD patterns of SnO_2 nanopowders at w_0=8 and w_0=10 are inserted in Figure 3 (a) and 3(b) with planes and pointed out the direction of crystallite growth is along planes (110), (101), (200), (111), (211), (220) and (301) observed at approximately 26.6^0, 33.9^0, 37.0^0, 37.9^0, 51.8^0, 54.7^0 and 65.0^0 respectively which were excellent coincide with cassiterite standard JCPDS pattern file no. 01-070-6153 of tetragonal crystalline structure of pure SnO_2 nanopowders and commercial sample SnO_2 characterization [20]. Patterns from (111), (220) are weak due to signal to noise and low intensities. Author was not found other phases and thus confirmed formation of phase pure SnO_2 nanopowders by XRD. Broad peaks were observed in the XRD pattern for small size nanopowders at w_0=8 compared to large nanopowders at w_0=10 as a result of the smaller crystallite size, along with sharp peaks which bring forth the finest crystalline nature of average crystalline size was calculated from Debye Scherrer equation [23]:

$$D = K\,\lambda\,(A^0) / \beta\,(2\theta)\cos\theta \qquad (2)$$

Where, D is the average crystalline size, K is the shape factor equal to 0.9, λ is the X-ray wavelength equal to 1.54060 A^0, θ is the Bragg diffraction angle of the peak in degree.

And β is the full width at half maximum (FWHM) for peak broadening in 2θ unit..

When measuring FWHM using OriginPro software, its value was in 2θ (e.g. if measuring value 26.6748 in degree, then 2θ = 26.6748 = β), but during determination of average crystalline size, its value must be converted to radians (1 rad = 180 ×7/22 0r 180/π).

Now,

For plane (110) at 26.6^0, using OriginPro software,

$$\beta = 2\theta - \text{error} = 26.90956^0 - 0.65031^0 = 26.25925^0$$

$$= 26.25925^0 \times 22 / 180 \times 7 = 26.25925^0 / 57.273$$

$$= 0.4585\ \text{rad}$$

Therefore, $D = 0.9 \times 1.54060\ A^0 / 0.4585\ \text{rad} \times \cos(26.6^0/2)$

$$= 1.38654 / 0.4585\ \text{rad} \times \cos 13.3^0$$

$$= 1.38654 / 0.4585\ \text{rad} \times 0.97318$$

$$D = 3.10742\ A^0$$

$$D = 0.310742\ nm$$

The crystalline size of plane (110) is 0.310742 nm

Similarly,

For plane (101), D = 0.31614 nm

For plane (200), D = 0.3189 nm
For plane (211), D = 0.11821 nm
For plane (301), D = 0.12607 nm
Thus, average crystalline size of SnO_2 nanopowders at w_0 = 8,

= (0.310742 + 0.31614 + 0.3189 + 0.11821 + 0.12607) nm / 5

= 0.2380 nm

The SEM micrographs of SnO_2 nanopowders sizes at w_0=8 and w_0=10 are displayed in Figure 4. The addressed images trace uniformly spherical particle size distribution. Reverse Microemulsion Precipitation is the method to get nanopowders with size and shape controlled and uniformly distribution of desired sizes nanopowders but there was observed some relatively larger particle sizes with approximately same diameter because of agglomeration of aggregates during calcination at 600^0C about 4h and therefore, one cannot measure the particles size which is quite similar in shape with commercial sample and the prepared nanoparticles by microemulsion approach of prior literature [20, 24-25]. The findings was observed spherical morphology with average particle size 153.242 nm and 131.604 nm and an average diameter 8.02 nm at w_0=8 and 10.01 nm at w_0=10 respectively by analysis SEM image using Imagej software. Histograms are put in Figure 5 and the higher specific surface area was to be observed 107.731 m^2/ g (count 637) of small nanopowders at w_0=8 and that of 86.314 m^2/ g (count 341) for relatively larger at w_0=10 which is obviously more than conventional Reverse Microemulsion Method [1] are well agreement with XRD result.

Total surface area

$$S\ A = N.\ Sa \tag{3}$$

For spherical nanopowders $Sa = 4\ \pi\ r^2$
Thus at diameter 8.02 nm, $Sa = 4\ \pi\ (4.01\ nm \times 10^{-9})^2\ m^2$

$$= 4\ \pi\ (4.01)^2 \times 10^{-18}\ m^2$$

Small volume, $v = 4/3\ \pi\ r^3 = 4/3\ \pi\ (8.02 / 2)^3$ nm = $4/3\ \pi\ (4.01)^3 \times (10^{-7})^3\ cm^3$

$$v = 4/3\ \pi\ (4.01)^3 \times 10^{-21}\ cm^3$$

And

$$N \times v = V \tag{4}$$

$N = V / v = 1\ g / 6.95\ g/cm^3 /$ v particles
$N = 0.144\ cm^3$ / v particles
$N = 0.144\ cm^3 / 4/3\ \pi\ (4.01)^3 \times 10^{-21}\ cm^3$ particles
$= 0.432 / 4\ \pi\ (4.01)^3 \times 10^{-21}$ particles
Therefore, Total surface area, S A = N × Sa

$$= 0.432 / 4\ \pi\ (4.01)^3 \times 10^{-21} \times 4\ \pi\ (4.01)^2 \times 10^{-18}\ m^2$$

$$= 107.731\ m^2$$

Specific surface area = 107.731 m^2 / g in case of diameter 8.02 nm

The characteristic FTIR for standard SnO_2 generally shows stretching bands with vibrations at 663 cm^{-1} corresponds to the Sn-O of Sn-O-Sn stretching vibrations and observed peak around this peak when characterized commercial SnO_2 nanopowders [20]. The FTIR transmission spectrum of SnO_2 nanopowders at w_0=10 after calcination is allowed to Figure 6 which illustrates that the peak at 678.94 cm^{-1} is the stretching vibration mode of surface bridging oxide Sn-O of Sn-O-Sn. There were no peaks observed in the ranges 3300-3430 cm^{-1}, 1635-1619 cm^{-1}, 2922 cm^{-1}, 2841 cm^{-1} and 1400 cm^{-1} indicating no presence of -OH groups of water, C-H groups and –NH- groups respectively on the surface of calcined SnO_2 nanopowders. These results were found to be good consent with the standard and published literatures [2, 8, 26].

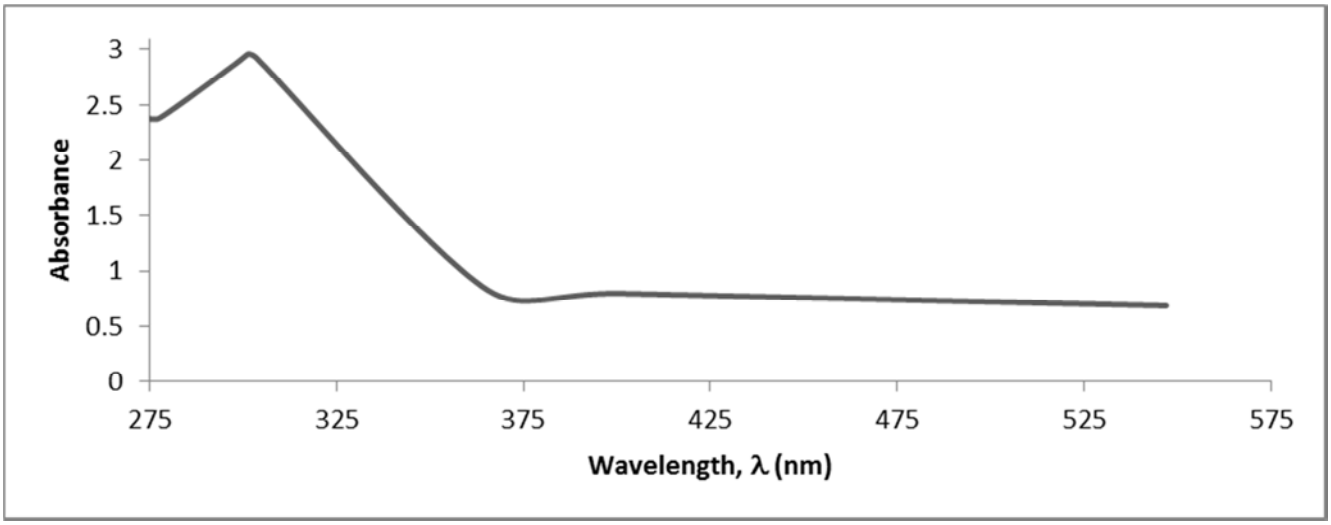

Figure 1. *The UV-Visible spectrum of 2SnO2.4H2O nanoparticles in solution at w0=8.*

Table 2. *The calculated values for Tauc Plot from UV-Vis measurement.*

No.	Wavelength, nm	Absorbance	hυ, eV	$(\alpha h\upsilon)^2$, eV^2cm^{-2}
1.	241.80	2.70	5.1282	191.7156
2.	243.90	2.704	5.0840	188.9800
3.	245.80	2.697	5.0447	185.1096
4.	247.30	2.678	5.0141	180.3111
5.	261.30	2.539	4.745	145.1302
6.	277.80	2.383	4.464	113.1670
7.	365.30	0.829	3.394	7.9180
8.	401.4	0.795	3.0892	6.0319
9.	547.0	0.684	2.267	2.4056

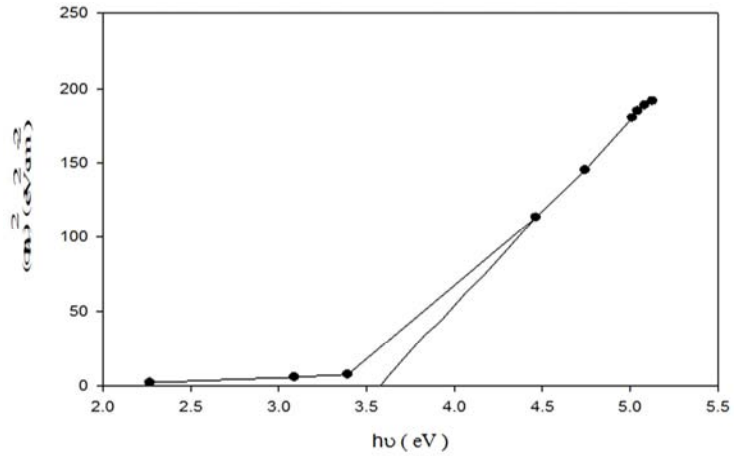

Figure 2. *$(\alpha h\mu)2$ Versus $h\upsilon$ for $2SnO_2.4H_2O$ nanoparticles at $w_0=8$.*

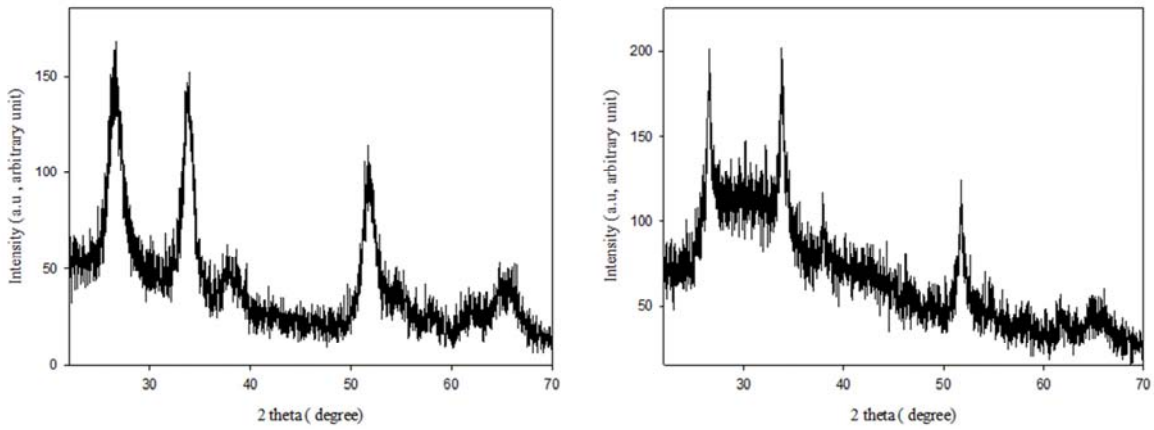

Figure 3a. *XRD patterns of SnO_2 nanopowders at $w_0=8$ and $w_0=10$.*

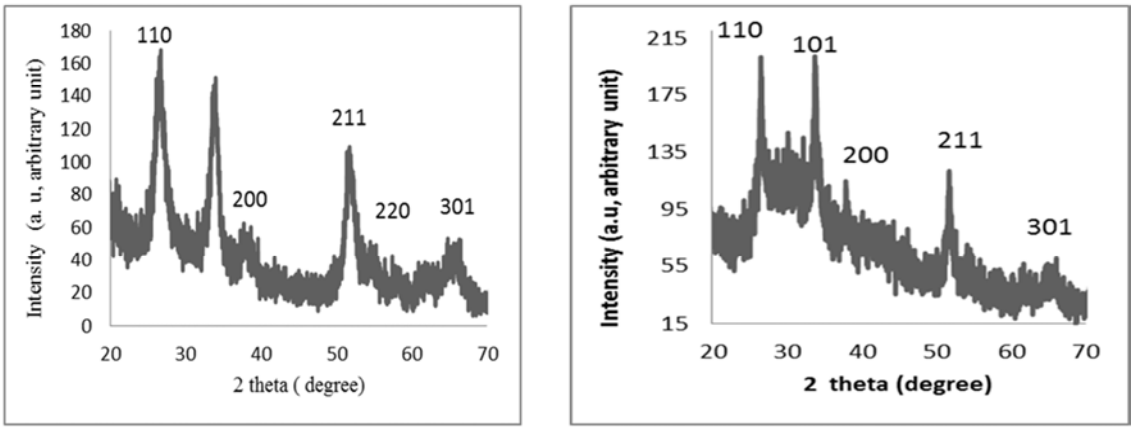

Figure 3b. *XRD patterns of SnO_2 nanopowders at $w_0=8$ and $w_0=10$ indicating planes.*

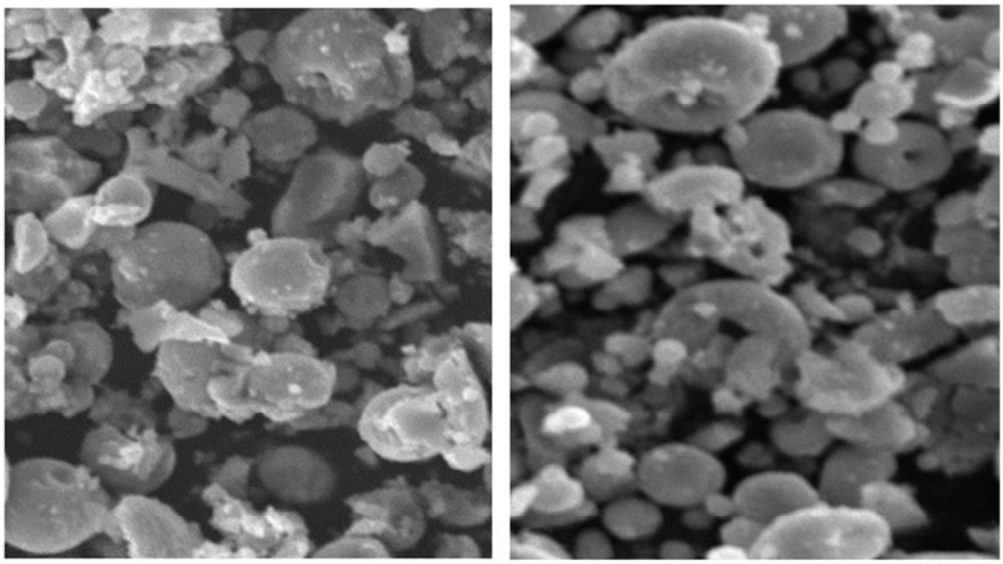

4(a): diameter 8.02 nm 4(b): diameter 10.01 nm

Figure 4. *SEM micrographs of SnO2 nanopowders sizes at diameter 8.02 nm and 10.01 nm.*

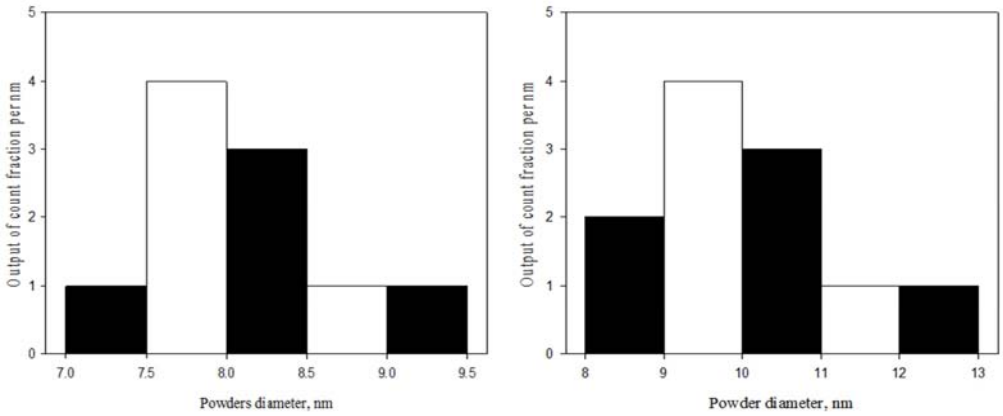

Figure 5. *Histograms of SnO2 nanopowders at diameter 8.02nm and 10.01 nm.*

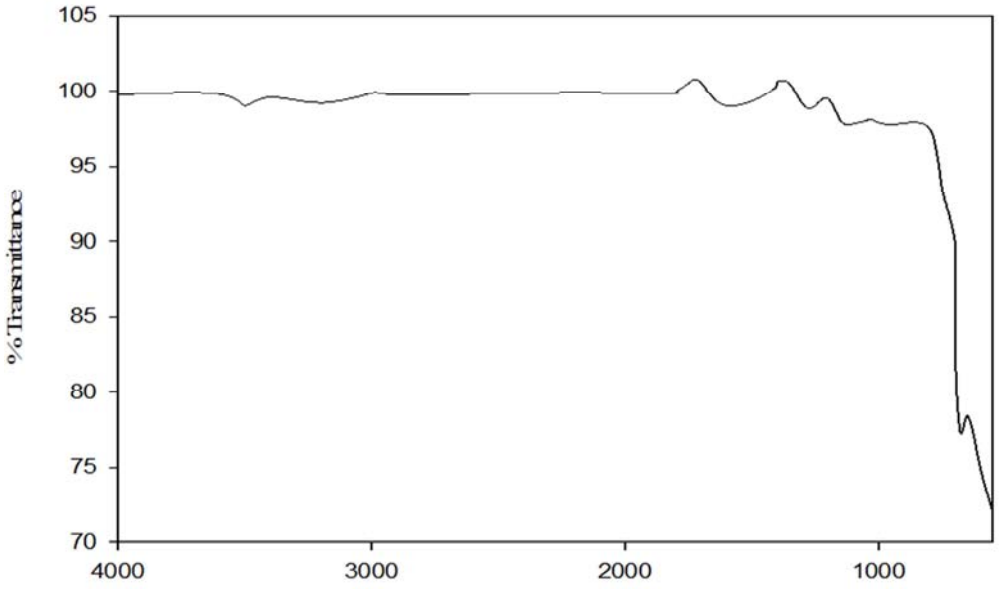

Figure 6. *The FTIR spectrum of SnO2 nanopowders at w0=10 calcination at 6000C.*

4. Conclusions

Size controllable nano dimension SnO_2 powders synthesis method development has been major concerned in the last decades. "Reverse Microemulsion Precipitation" method was developed, characterized and found to be nanosized synthesized powders after reported literature for advanced ceramics, structural materials and sensor materials and so on. UV-Visible Spectrophotometer results demonstrate $2SnO_2.4H_2O$ nanoparticles in solution in the UV range exhibit an intense characteristic peak at 303.4 nm and absorption edge between 321.6-371.6 nm and in the visible range optically transparent. XRD patterns give the phase pure tetragonal crystalline structure of SnO_2 nanopowders and average crystalline size 0.380 nm for microemulsion at w_0=8. The SEM image found to be described the spherical shape and average particle size 153.242 nm (count 637) and 131.604 nm (count 341) and average diameter nm 8.02 nm and 10.01 nm at w_0= 8 and at w_0=10 respectively of the SnO_2 nanopowders. FTIR record confirms only existence stretching band of oxide Sn-O of Sn-O-Sn at 678.94 cm^{-1} of prepared SnO_2 nanopowders by "Reverse Microemulsion Precipitation.

Acknowledgements

Author is grateful and delighted to thanks to Bangladesh Council of Scientific and Industrial Research for funding to carry out this research work and PP & PDC for XRD, INARS for FTIR and UV-Visible Spectrophotometer, BCSIR Laboratories, Dhaka for SEM measurement respectively.

References

[1] Jong H. K. and Ki C. Song, Preparation of Nanosize Tin Oxide Particles from Water-in-Oil microemulsions, J of Collo and Inter Sci. (1999), 212: 193-196.

[2] Boon-Tech H, M. A. Farrukh and Rohana A, Surfactant-controlled aqueous synthesis of SnO2 nanoparticles via the hydrothermal and conventional heating methods, Turk J Chem. (2010), 34: 537-550.

[3] Abdullah M. S, A. N. Naje and Azhar S. N. (2013), Preparation and Characterization of SnO2 Nanoparticles, Inter J of Innov Resea in Sci, Eng and Tec. (2013), 2(12): 7068-7072.

[4] A. M. EL-Rafei, H. Youssef and N. M. Ahmed, J. Ceram Sci Tech. (2014), 05(03): 217-222.

[5] Belin S. et al., Preparation of ceramic membranes from surface modified tin oxide nanoparticles, Colloids and Surfaces A-physicochemical and Engineering Aspects. Amsterdam: Elsevier B.V. (2003), 216 (1-3): 195-206.

[6] A. bcc Research, Advance Ceramics and Nanoceramic powders, NANO015F. (2011).

[7] Alreza R, Mehedi A, S. M. Amininzhad, Sayed A. and Sajjad R, The Antibacterial Activity of SnO2 Nanoparticles against Esherichia coli and Staphylococcus aureus, Zahedan J. Res Med Sci. (2015), 17(9): e1053.

[8] A. J. Novinrooz, A. Taherkhani and Y. rezainik, Making a nanosensor sensitive to CO gas with SNO2 Nanopowder prepared by One-Step Solid State synthesis method, J Basic Appl Sci Res. (2013), 3(2s): 1-5.

[9] Li G J and Kawi S, Mater Lett. (1998), 34:99.

[10] A. P. Maciel, C. O. Paiva-Santos, E. Longo, P. N. Lisboa-Filho and W. H. Schreiner, Microstructural and morphological analysis of pure and Ce-doped tin dioxide nanoparticles, J Euro Cera Soci. (2003), 23: 707-713.

[11] A. Mhemdi, K. Omri, R. Bargougui and S. Ammar, Synthesis and characterization of SnO2 nanoparticles: Effect of hydrolysis rate on the optical properties, Adv Mater Lett. (2015), 1-8.

[12] Adnan R, Farrukh M. A, Rahman I. A. and Razana N. A, J. Chin. Chem. Soc. (2010), 57: 222-229.

[13] A. Youssefic, M. M. Bagheri-Mohagheghia,b, M. R. Alinejada, M. Shokooh-Saremid and N Shahtahmasebia, The effect of the post-annealing temperature on the nano-structure and energy band gap of SnO2 semiconducting oxide nano-particles synthesized by polymerizing–complexing sol– gel method, Physica B. (2008), 403: 2431–2437.

[14] Dongwook S, Y. Kim and Yougsub Y, Electrochemical characteristics of tin oxide and tin/tin oxide composite powder synthesized by aerosol flame deposition, J Cera Proc Res. (2010), 11(6): 673-677.

[15] Kang Y. and Song K, Mater. Lett. (2000), 42: 283-2893.

[16] Aguilar-Elguezabal A, Antúnez-Flores W, Ascencio J. A, Diaz R, Miki-Yoshida M, Paraguay-Delgado F and Santiago P, Structural analysis and growing mechanisms for long SnO2 nanorods synthesized by spraypyrolysis, Nanotechnology. (2005). 16: 688.

[17] Y. Wang and J. Y. Lee, Molten Salt Synthesis of Tin Oxide Nanorods: Morphological and Electrochemical Features, J Phys Chem B. (2004), 108: 17832-17837.

[18] C LIU, Guang-ping LI, Xue CAO, Yong-chun SHU and Yong-neng HU, Integrated process of large-scale and size-controlled SnO2 nanoparticles by hydrothermal method, Trans. Nonferrous Met. Soc. (2013), 23: 725-730.

[19] H X Yang, J. F. Qian, X. P Ai and Y. L. Cao, J Phys Chem. (2007), 111: 14067.

[20] B. A. Dedavid, M. J. Pires and R. C. Abruzzi, Characterization of tin dioxide nanoparticles synthesized by oxidation, Ceramica. (2015), 61: 328-333.

[21] Y. Zang and A. Shakouri, Lab 8: Optical Absorption, Spring. (2002), 1-9.

[22] B. Streetman, EE. 128- Solid-State Electronic Devices. 4 th Edi. (Prentice – Hall) 1995, Chapter 4.1.

[23] Cullity B D, Elements of X-ray Diffraction, Boston, Addison-Wesley, Publishing Co. (1956).

[24] M. E. EL-Hefnawy, Water in Olive Oil Surfactantless Microemulsions as Medium for CdS Nanoparticles Synthesis, Modern Applied Science. (2012), (4): 101-105.

[25] A. Gaber, M. A. Abdel-Rahim, A. Y. Abdel-Latief and M. N. Abdel-Salam, Influence of Calcination Temperature on the Structure and Porosity of Nanocrystalline SnO2 Synthesized by a Conventional Precipitation method, Int J Electrochem Sci. (2013), 9: 81-95.

[26] A. Akbari, A. Talebi, E. Taleb and S. Tazikeh, Synthesis and characterization of tin oxide nanoparticles via the Co-precipitation method, Materials Science-Poland. (2014), 32(1): 98-101.